Starch
www.starch-journal.com

Role of Endogenous Protein in the Spherical Aggregation of Taro Starch Granules upon Spray-Drying and in In Vitro Digestibility

Eduardo Jaime Vernon-Carter, Jose Alvarez-Ramirez, Luis A. Bello-Perez, Carmen Hernandez-Jaimes, and Isabel Reyes*

The role of endogenous protein in the formation of spray-dried taro starch spherical aggregates is studied in this work. Taro starch dispersions (30 g per 100 mL water) are added with different protease concentrations (0.0, 1.0, and 5.0×10^3 IU protease per g starch) for degrading the surface protein of the starch granules. Protease treatment has a negative effect on the formation of starch aggregates, which are scarce and irregular. The incorporation of exogenous protein in the form of whey protein isolate (WPI) improved the formation of starch aggregates, but with non-spherical morphology. Fourier transformed infrared (FTIR) analysis reveals that the formation of random structures at the expense of β-structures (up to 65%) in proteins is the mechanism responsible for the spherical aggregates formation. In vitro digestibility tests show that spherical aggregates are less digestible (≈19% of RDS) than native taro starch (≈40% of RDS), an effect that might be attributed to increased ordering and crystallinity (≈34% for spray-dried starch) induced by thermal modifications in the spray-drying process.

1. Introduction

Zhao and Whistler[1] reported that spray-dried starch dispersions of commercial amaranth starch resulted in the aggregation of the starch granules with an unique spherical shape. A more detailed analysis revealed that small starch granules had the ability to form spherical aggregates when spray-dried in the presence of small amounts of binding agents, such as proteins or water-soluble polysaccharides.[2] It was proposed that these structures could be used as carriers for flavors and other active compounds. Ever since, this issue has attracted the attention of researchers interested in innovative microencapsulation systems. Many authors have demonstrated that the formation of spherical aggregates is mediated by the addition of binding agents (e.g., proteins and polysaccharides). Tari et al.[3] obtained spherical aggregates from amaranth, rice, quinoa, and colocasia starches using gum Arabic, carboxymethyl cellulose (CMC) and carrageenan as binding agents. The spherical aggregates were appropriate for encapsulating flavor compounds (e.g., vanilla). Beirao-da-Costa et al.[4] showed that CMC and gelatin were suitable for promoting the formation of spherical aggregates from rice starch, and that intraparticle porosity was mainly dependent on the concentration of the biopolymers.

More recently, Gonzalez-Soto et al.[5] reported that taro starch had the ability to form spherical aggregates without the addition of binding agents. It was postulated that the endogenous protein (about 5–7 g per 100 g flour) acted as binding agent by forming crosslinked structures between the starch chains. The potential of taro starch spherical aggregates as wall material for the microencapsulation of bioactives by spray-drying was studied by Hoyos-Leyva et al.[6] Nevertheless, despite all of the above, the role of the endogenous protein on the formation of spherical aggregates has not been clarified. Studies on insoluble remnants (i.e., ghosts) obtained after granule gelatinization revealed that protein was concentrated on the swollen surface, and acted largely as granule-bound starch synthase.[7] Degradation of proteins by protease reactions indicated that endogenous proteins could be acting as aggregating agents of starch granules summing to the ghost integrity.[8] Recently, it was shown that neither integral nor surface proteins were crucial for integrity of starch ghosts.[9] These results indicate that surface proteins could be available in starch granules for the formation and stabilization of granular structures induced by the spray-drying process.

The aim of this study was to gain systematic insights on the effect of endogenous protein added to taro starch dispersions on the formation of spray-dried spherical aggregates. To this end, the taro flour was subjected to protease treatment for disrupting the protein contained in the taro flour and assesses the

E. J. Vernon-Carter, J. Alvarez-Ramirez
Departamento de Ingeniería de Procesos e Hidráulica
Universidad Autónoma Metropolitana, Iztapalapa
Apartado, 55–534, Iztapalapa, CDMX, C.P. 09340, México
L. A. Bello-Perez
CEPROBI. km 6 Carr. Yautepec-Jojutla
Calle Ceprobi No. 8, Apartado Postal 24, Yautepec, Morelos 62731, México
C. Hernandez-Jaimes, I. Reyes
Universidad Autónoma del Estado de México
Campus El Cerrillo, Toluca 50200, México
E-mail: chj@uaem.mx; carmenhernandezjaimes@gmail.com
The ORCID identification number(s) for the author(s) of this article can be found under https://doi.org/10.1002/star.201900087

DOI: 10.1002/star.201900087

concomitant effect on the structure of spherical aggregates. Also, the in vitro digestibility of the spray-dried spherical aggregates was quantified and compared with the digestibility properties of native starch from taro flour.

2. Experimental Section

2.1. Materials

Taro starch (TS) was prepared following the procedure reported by Gonzalez-Soto et al.[5] Protease from *Bacillus licheniformis* (2.4 IU per g), pancreatic α-amylase type VI-B from porcine pancreas (EC 3.2.1.1, A3176), amyloglucosidase (EC 3.2.1.3, A7095), were purchased from Sigma-Aldrich (St. Louis, MO, USA).

2.2. Composition Analysis

Ash, protein, and fat were analyzed according to AACC-2000 methods 08-01, 46-13, and 30-25, respectively.

2.3. Preparation of Spherical Aggregates

Thirty grams of TS were dispersed in 100 mL of water. The dispersion was stirred gently for 30 min at room temperature. To disrupt the protein structure on the taro starch granules and assess the effect in the formation of spherical aggregates, the TS dispersions were treated with 0.0, 1.0×10^3, and 5.0×10^3 IU protease per g starch in carbonate buffer (0.02 M, pH 9.0) at 36 °C for 60 min. The resulting dispersions were fed to a Mini Spray Dryer (Model B-290, BÜCHI UK Ltd, Chadderton, UK) equipped with a double flow atomizer. The drying conditions were the same used by Gonzalez-Soto et al.,[5] that is, inlet temperature of 145 °C, outlet temperature of 80 °C and flow rate of 7.6 mL min^{-1}. The dried powders were put into desiccators with a silica-gel bed at the bottom as desiccant, until required for analysis.[10] Samples were tagged as SD-x, where "x" denotes the amount of protease used for treatment. To contrast the results, the untreated taro starch dispersion was supplemented with 2 g WPI per 100 g starch, and spray-dried under the same conditions described above, and tagged as SD-WPI.

2.4. Particle Size Distribution

The mean particle size and size distribution (PSD) of the untreated taro starch (TS) and of the spray-dried (SD_x and SD-WPI) treatments were determined by laser diffraction analysis (Mastersizer 2000, Malvern Instruments Ltd., Malvern, Worcestershire, UK). The samples were analyzed using the Hydro 2000S accessory. The powders were diluted in water to achieve saturation between 14 and 16% (concentration of ≈0.001%), and sonicated (250 rpm for 2 min) during the analysis to avoid aggregation of the starch granules.

2.5. Light Microscopy

A polarized light microscope (Eclipse 80i, Nikon, Japan) equipped with a 40× objective lens and a digital camera (Digital imaging Head, DC330 camera MTI, Japan) was used. The dried starch was spread on a slide and a coverslip was added to the slide. A drop of deionized water was added to the edge of the coverslip and the images were captured under polarized light. Selected micrographs are presented.

2.6. Scanning Electron Microscopy

Starch samples were fixed to conductive tape mounted on a brass disc. Samples were then coated with gold using Polaron E5100 sputter coater (Polaron Equipment Ltd, Watford, UK). Images of starches were captured using a scanning electronic microscope model JSM-5800LV (JEOL, Tokyo, Japan) at magnification of 3000×. Selected micrographs are presented.

2.7. X-Ray Diffraction Analysis

X-ray diffraction (XRD) patterns were obtained using a Rigaku diffractometer, model MiniFlex600 (Rigaku Corporation, Tokyo, Japan). The moisture content of the samples was adjusted to 86% by storing the samples in a glass desiccator with a saturated potassium sulfate solution for seven days at room temperature.[11] The range of the scanned diffraction angle (2θ) was 2° to 60° and the scanning speed was 2° per min.

2.8. Fourier Transformed Infrared Analysis

Fourier transformed infrared (FTIR) analysis was carried out in a Vertex 70 FT-IR (Bruker Optik GmbH, Ettlingen, Germany) spectrometer equipped with a mercury cadmium telluride detector and KBr beam splitter using a Platinum Diamond ATR accessory with a diamond crystal at an angle of incidence of 45°. Spectra were collected using 256 scans at 4 cm^{-1} resolution over the entire 4000–400 cm^{-1} wavenumber region. Two spectra were collected for each sample and averaged. The analysis was performed using OPUS version 7.0 software.

2.9. In Vitro Starch Digestibility

Total starch content was determined by using a 50 mg sample dispersed in 2 M KOH to hydrolyze all the starch (30 min). The resulting dispersion was incubated (60 °C, 45 min, pH 4.75) with amyloglucosidase. The glucose content was then determined using the glucose oxidase/peroxidase (GOD/PAD) assay (SERA-PAK_Plus, Bayer Mexico SA de CV). Total starch content was calculated as glucose (mg) × 0.9. For digestibility tests, 3 g of sample was dispersed in 40 mL sodium acetate buffer (0.2 M, pH 6.0) in a 95 °C water bath according to optimum cooking time and cooled down to 37 °C. Artificial saliva containing porcine α-amylase (250 IU mL^{-1} of carbonate buffer, pH 7) and pepsin

(1 mg mL^{-1} in 0.02 M HCl, pH 2) was used. The mixture was incubated at 37 °C for 30 min. The digestion was performed with a mixture of pancreatin (2 mg mL^{-1}) and amyloglucosidase (28 IU mL^{-1}) in water. Aliquots were taken at the time intervals of 5, 10, 15, 20, 30, 40, 50, 60, 90, 120, 240, and 360 min before addition of 300 µL of stop solution (0.3 M Na_2CO_3) to prevent further amylase activity. After centrifugation (2000 × *g* for 5 min), the glucose concentration in the supernatant was determined using a D-Glucose Assay Kit (GOPOD Format from Megazyme, International, Bray, Ireland). The results were presented as percentage of hydrolyzed starch. The rate of enzymatic starch digestion was described by means of the first-order exponential decaying model:[12]

$$X(t) = \left(1 - e^{-k_H t}\right) X_\infty \quad (1)$$

where k_H is the hydrolysis rate constant, $X(t)$ is the hydrolyzed starch fraction, and X_∞ is the limiting hydrolyzed starch fraction. The rapidly digestible starch (RDS) content was measured as the amount of glucose released in 20 min of incubation. The slowly digestible starch (SDS) fraction was defined as the fraction digested between 20 and 120 min of hydrolysis. The starch not hydrolyzed within 120 min was designated resistant starch (RS) content.

2.10. Statistical Analysis

The results are presented as the mean ± SE (standard error) of three or more replicates. One-way analysis of variance (ANOVA) was used to evaluate the difference among means with a significance level of $\alpha = 0.05$ using the Minitab 15 statistics package (Minitab Inc., State College, PA, USA).

3. Results and Discussion

3.1. Composition Analysis

The chemical composition of native TS was 8.4 g moisture per 100 g, 0.4 lipid per 100 g, 74.2 g starch per 100 g, and 7.5 g protein per 100 g. Early reports indicated that taro proteins exhibited five patterns for major cultivars, as revealed by gel electrophoresis.[13,14] It was also reported that taro starch proteins of major cultivars are of tarim type as identified by mass spectroscopy. In turn, this implies that taro protein is in the form of G1a/G1d isoforms.[15] The protein content of SD-0 decreased to 7.3 g per 100 g after spray-drying of TS. The protease treatment produced an important reduction of the protein content, with values of 6.5 g per 100 g for DS-1 and 3.2 g per 100 g for DS-5. This result indicates that the protease treatment effectively disrupted the endogenous protein of taro starch. If protein content is important in the formation of spherical aggregates, then DS-1 and DS-5 should have different effect on the morphology spray-dried aggregated particles. The same should occur in the case of DS-WPI, which had a total protein content of 10.3 g per 100 g.

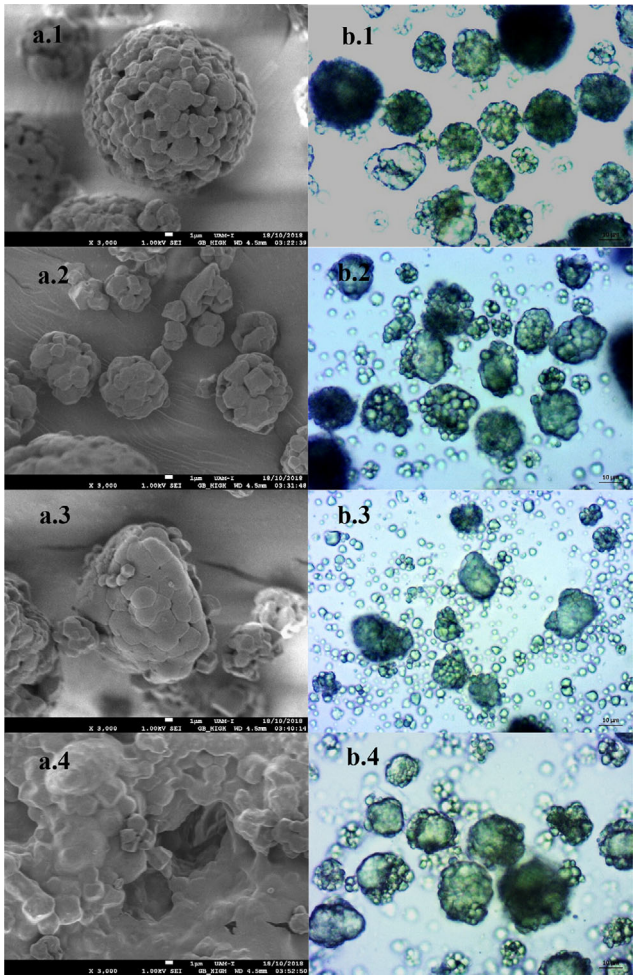

Figure 1. SEM micrographs at magnification of 3000× (a, left panel) and light micrographs at magnification of 40× (b, right panel) for the spray-dried taro starch treatments: 1) SD-0 (without added protease); 2) SD-1 (treated with 1000 IU protease per g starch); 3) SD-5 (treated with 5000 IU protease per g starch); and 4) SD-WPI (TF starch added with whey protein isolate).

3.2. Light Microscopy and Scanning Electron Microscopy Images

The morphology the spray-dried taro starch (SD-0) is illustrated by the scanning electron microscopy (SEM; **Figure 1**a1) and light (Figure 1b1) micrographs. In both cases, it can be observed that the starch granules were aggregated into spherical, porous structures, resembling popcorn balls.[5] Importantly, the formation of these aggregates was induced without the mediation of an external binding agent. The treatment with protease affected the formation and morphology of taro starch aggregates. Figure 1a2,b2 (SD-1) shows that although aggregates were still formed, they began to display slight deviations from spherical morphologies. This effect was more pronounced for SD-5 (Figure 1a3,b3), which was added with higher protease concentration. Not all of the starch granules formed aggregates, with a large number of then occurring individually (Figure 1b3). When starch granules did aggregate, their morphology was characterized by irregular shapes, covered by a layer formed probably by starch chains that leached

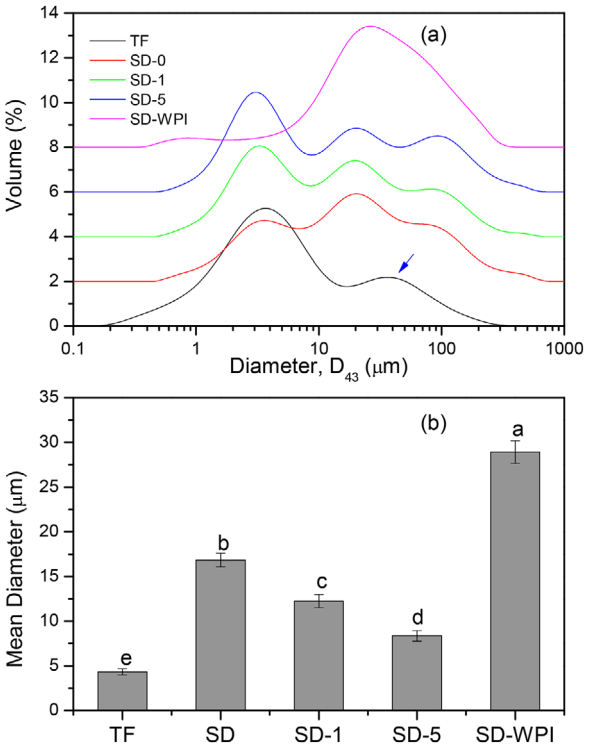

Figure 2. a) Particle size distribution of the taro flour (TF) and the different spray-dried (SD) samples. b) Mean particle diameter obtained from the particle size distribution.

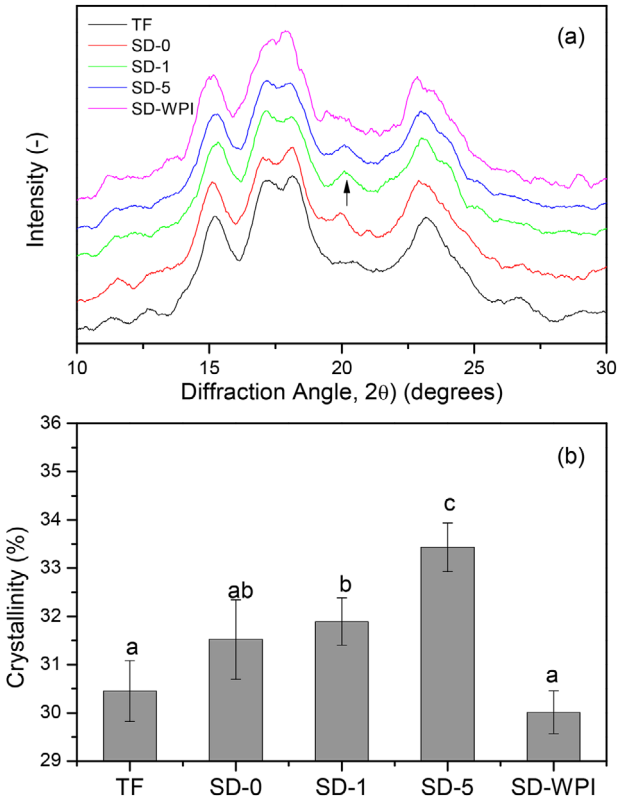

Figure 3. a) X-ray diffraction pattern of the taro flour (TF) and the different spray-dried (SD) samples. b) Relative crystallinity estimated from the XRD pattern.

out during spray-drying (Figure 1a3). Thus, it may be inferred from these results that indeed the endogenous protein of TS played an important role as binding agent in the formation of spherical aggregates. As a matter of fact, it may be observed in Figure 1a4,b4 that the addition of exogenous protein in the form of WPI to TS (SD-WPI) promoted the formation of large aggregates upon spray-drying, although their morphology was irregular. This suggests that WPI acted as binding agent, although with poor ability for forming regular structures.

3.3. Particle Size

The particle size distribution and mean particle size of the native TS and the spray-dried treatments are shown **Figure 2**a,b, respectively. The distribution of TS was bimodal with a large peak at about 4 μm, and a second larger peak at about 45 μm. After spray-drying treatment (SD-0), the PSD became multimodal, shifting to the right to higher diameters, due to the formation of spherical aggregates (Figure 1a2,b2) of different sizes. Besides the small peak at about 4 μm, two large peaks at about 20 and 90–100 μm were obtained. When TS was treated with protease (SD-1 and SD-5), PSD remained multimodal, but the predominant distribution peak was shifted to the left to smaller particle diameters, the higher the protease concentration, the further to the left was the shift. This suggests that the formation of aggregates was reduced as consequence of the disruption of the endogenous starch protein (Figure 1a2,a3,b2,b3). On the other hand, the incorporation of exogenous WPI protein led to an important shift to larger diameters. In fact, SD-WPI was basically monomodal with the peak occurring at about 30–40 μm. As already observed in Figure 1a, the spray-drying process increased the mean particle diameter (Figure 2b), which was linked to the formation of particles aggregates. However, the protease treatment had a negative impact on the mean particle diameter, suggesting that the protein contained in TS had an important role in the formation of the spray-dried particle aggregates. Interestingly, the addition of WPI led to an important increase of the mean particle diameter (≈30 μm).

3.4. XRD Analysis

X-ray diffraction patterns of TS and the four different spray-dried samples (SD-0, SD-1, SD-5, and SD-WPI) are shown in **Figure 3**a. Diffraction peaks at 2θ of 15°, 17°, 18°, and 23° were detected for all the samples, indicative that the native and spray-dried taro starches can be classified as A-type. Thus, it may be inferred that the spray-drying process did not change the crystalline structure of the taro starch granules. A small peak at 20° also appeared in the samples, which is indicative of the V-type crystallinity usually associated with the presence of amylose-lipid complexes.[16] The strength of this peak increased with the spray-drying treatment, suggesting that spray-drying promoted the further formation amylose-lipid complexes. It is noted that the V-type peak at 20° also appeared for the sample SD-WPI, although not

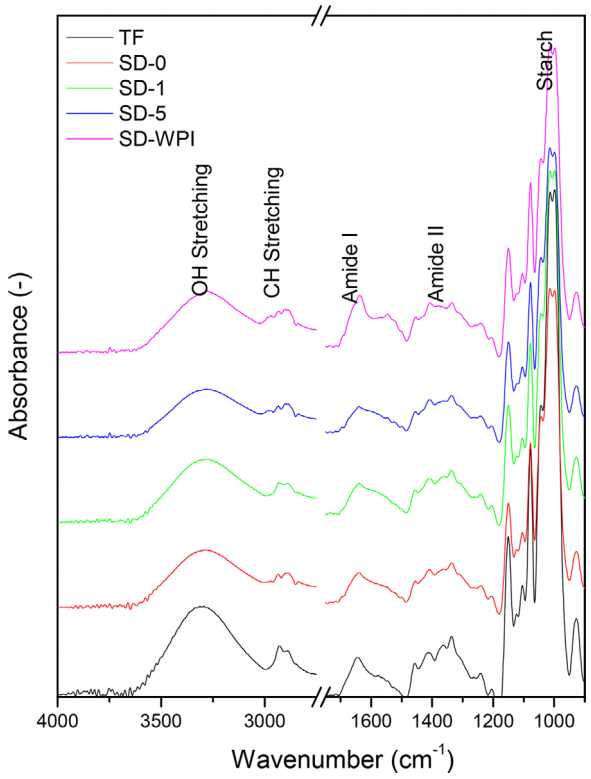

Figure 4. FTIR spectrum of the taro flour (TF) and the different spray-dried (SD) samples.

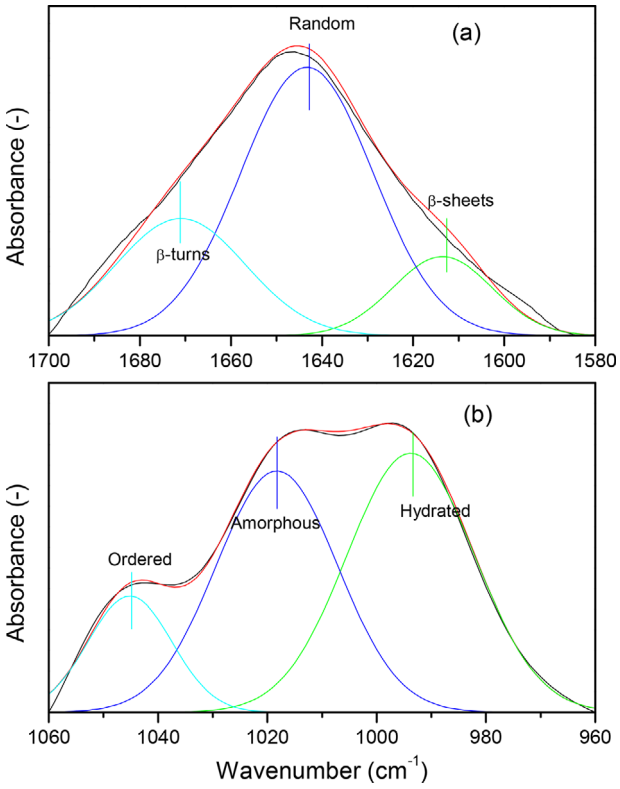

Figure 5. Example of deconvoluted FTIR spectrum in the a) Amide I, and b) starch fingerprint regions.

well-defined. In fact, the peak extended over a band in the range 19.5–20.5°, a masking effect caused probably by the WPI added that covers partially the granule surface. It has been shown that the presence of amylose-lipid complexes can slow down the enzymatic digestion of starch granules,[17] an effect that may be caused by the ability of this type of complexes to physically inhibit the access of digestive enzymes to the starch chains.[18] The relative crystallinity of the starch samples is shown in Figure 3b. Although the protease treatment increased the relative crystallinity, its impact was small as the relative crystallinity increased only from 30.5% to values not higher than 33.0%.

3.5. FTIR Analysis

The FTIR spectrum for the TS is presented in **Figure 4**. The wide band in the range 3600–3000 cm^{-1} has been ascribed to OH stretching, which in turn is linked to intramolecular hydrogen bond. In general, this band reflects hydrated molecular structures mediated by hydrogen bonds.[19] After spray-drying, the peak of this band was shifted from 3385 cm^{-1} to about 3360 cm^{-1}, which indicated the redistribution of water molecules within the TS molecular structure. The small band at about 2930 cm^{-1} is attributed to CH-stretching. The band in the range 1700–1600 cm^{-1} corresponds to the Amide I group, linked to the protein contained in the TS. This band exhibited a prominent peak at 1636 cm^{-1}, which was modified by the effect of the spray-drying process, reflecting conformational changes of the protein chains.[20,21] A second protein band was displayed in the range 1500–1200 cm^{-1}, reflecting the Amide II group. The structure of this band was not affected by spray-drying. The band showing the largest intensity was that at about 1100–950 cm^{-1}, which is ascribed to (COC and C—O) polysaccharide vibrations. In particular, this band is linked to molecular vibrations of starch molecular groups.

It has been postulated that the formation of spherical aggregates involves the interactions between starch and proteins.[5] Figure 4a shows that e spray-drying modified the molecular organization of starch and proteins. A more systematic analysis of the Amide I and starch fingerprint regions should provide valuable insights regarding the structural changes undergone by starch and proteins upon spray-drying and during the formation of the spherical aggregates. Both, the Amide I and carbohydrates bands are composed by overlapping individual effects. In this way, numerical deconvolution of these bands was carried out for recasting the individual contributions. **Figure 5** illustrates the results of the deconvolution of the Amide I and carbohydrates fingerprint regions. For the Amide I region (Figure 5a), the peak at about 1671 cm^{-1} denotes β-sheet structures, the peak at 1640–1645 cm^{1} is linked to random structures, and the peak at 1614–1610 cm^{-1} to β-turns. For the starch region (Figure 5b), the peak at about 1047 cm^{-1} has been linked to ordered structures, and the peak at about 1022 cm^{-1} to amorphous structures. On the other hand, the peak at 995 cm^{-1} reflects hydrated structures. The ratios $R_{1047/1022}$ and $R_{995/1022}$ have been proposed as indicators of ordered-to-amorphous and hydrated-to-amorphous starch structures.[21] The estimated values $R_{995/1022}$ are presented in

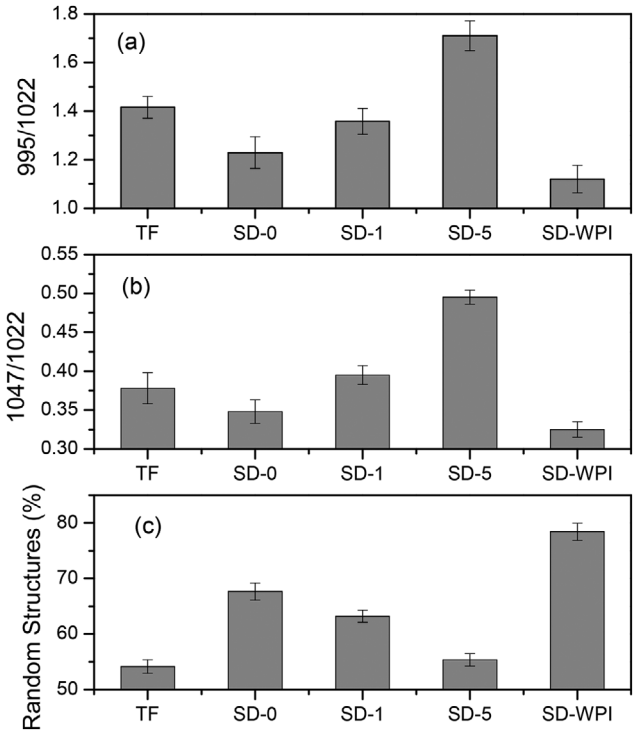

Figure 6. a) 995/10222, and b) 1047/1022 FTIR ratios estimated from deconvolution of the FTIR starch fingerprint region. c) Fraction of random structures obtained from deconvolution of the FTIR Amide I region.

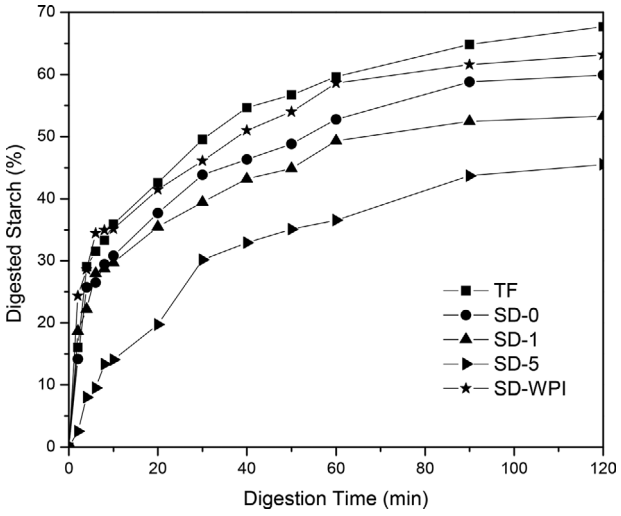

Figure 7. Enzymatic hydrolysis time courses of the different samples.

Figure 6a. Spray-drying decreased the value of $R_{995/1022}$ for SD-0, an expected result since the drying process likely redistributed the bound water molecules in the starch granule. However, the protease treatment (SD-1 and SD-5) increased the value of $R_{995/1022}$, suggesting that protein removal increased the hydration of the starch structures. The opposite effect was observed when exogenous protein was added to TS (SD-WPI), which presented the lowest $R_{995/1022}$ value. It is apparent that protein underwent important reconfigurations, which required taking water molecules from the starch structure. On the other hand, Figure 6b presents the ratio $R_{1047/1022}$, which reflects the ratio between ordered and amorphous starch structures. Interestingly, the behavior of the ratio $R_{1047/1022}$ followed a pattern similar to that of the ratio $R_{995/1022}$, which indicated that spray-drying reduced the ordered structures relative to the amorphous structures. However, the protease treatment (SD-1 and SD-5) led to an increase of the ordered structures. It is suggested that protein acted as a barrier to the heat transport, reducing in this way the transport of water and the thermal rearrangement of starch structures. Finally, Figure 6c shows that spray-drying and protease treatments had important effect in the structure of the protein. In fact, spray-drying of TS produced an important increase of the random structures of SD-0 at the expense of β structures. This suggests that random structures played an important role in the consolidation of the spherical aggregates obtained upon spray-drying. This postulate is sustained by the behavior of the random structures content in SD-1 and SD-5. In fact, the protease treatment induced a negative effect on the random structures. A further insight was revealed by the incorporation of exogenous protein. In fact, SD-WPI, which formed the largest aggregates, was the sample that presented the highest random structures content (about 80%).

3.6. In Vitro Digestibility

The time course of the enzymatic hydrolysis is shown in **Figure 7**. Starch digestibility of TS was reduced by the spray-drying (SD-0), and this effect was more pronounced when the TS was subjected to protease treatment (SD-1 and SD-5). In fact, the higher the protease concentration, the lower the maximum value of the hydrolyzed starch. FTIR analysis showed that spray-drying increased the value of $R_{1047/1022}$ (Figure 6a) which reflects the ratio of ordered-to-amorphous structures. In turn, ordered starch structures are less accessible to enzymatic actions, an effect that should be observed as reduced digestibility. Interestingly, the incorporation of exogenous protein in the form of WPI recovered partially the starch digestibility extent to SD-WPI. This is in line with the increased $R_{1047/1022}$ value exhibited by this treatment. It was suggested above that protein is distributed as an external layer covering the starch granules, as illustrated by SEM images in Figure 1a3. It is apparent that such layer acted as a heat transfer barrier, limiting the thermal rearrangement of molecular structures of the starch granule. In this way, the removal of the endogenous protein by protease action left partially or totally uncovered the starch granule, allowing an improved heat transport to the starch granule during the spray-drying. Surprisingly, studies on the effects of spray-drying on the starch digestibility are scarce. Recently, Zeng et al.[22] found that spray-drying slowed the digestibility of short-chain amylose crystals, probably due to the formation of compact starch structures.

The hydrolysis kinetics was numerically fitted by means of the exponential model given by Equation (1), and the estimated hydrolysis rate constant k_H is shown in **Table 1**. The results corroborate the findings of Figure 7, that is, that the combined effect of spray-drying and protease treatment slowed the enzymatic hydrolysis of the starch structures. In particular, the spherical

Table 1. Hydrolysis kinetics rate constant and starch fractions.

Sample	$k_H \times 10^2$ [min^{-1}]	RDS [%]	SDS [%]	RS [%]
TF	6.73 ± 0.21^b	43.84 ± 2.27^a	23.86 ± 1.16^b	32.30 ± 2.23^d
SD-0	6.24 ± 0.18^b	42.63 ± 1.76^a	17.28 ± 0.96^d	40.09 ± 1.73^c
SD-1	5.26 ± 0.16^c	35.46 ± 1.75c^b	17.83 ± 1.02^d	46.71 ± 1.97^b
SD-5	3.07 ± 0.16^d	19.74 ± 1.45^d	25.08 ± 1.52^a	54.46 ± 2.48^a
SD-WPI	6.62 ± 0.23^a	39.47 ± 1.76^b	22.69 ± 0.95^c	37.84 ± 2.03^{c,d}

Values are means ± standard error of three replicates; Superscripts with different lower-case letters at different concentrations indicate significant differences ($p \leq 0.05$); RDS, rapidly digestible starch; SDS, slowly digestible starch; RS, resistant starch.

aggregates obtained by applying only the spray-drying without protease addition (SD-0) were less digestible than the starch contained in TS. The aggregated structure and the increased molecular ordering detected by the FTIR analysis make less accessible the starch chains to enzymatic attack. The starch fractions in terms of the digestibility properties (RDS, SDS, and RS) were also shown in Table 1. The main effect of spray-drying was to reduce the RDS fraction and increase the RS fraction, accompanied by a marginal decrease of the SDS fraction. However, the protease treatment (SD-1 and SD-5) deepened the reduction of the RDS fraction, while increasing both the SDS and RS fractions. Finally, exogenous protein (SD-WPI), produced a significant reductions of RDS and SDS, and a significant increase in RS respect that of TS, probably because WPI covered the starch granules (Figure 1a4) and limited the hydrolysis kinetics.[23]

3.7. Discussion

Recent reports have shown that spherical aggregates are stable structures that can be used for microencapsulation of active compounds.[6,11] However, the mechanisms involved in the formation of spherical aggregates via spray-drying are not clear at all. Accurate understanding of the formation of spherical aggregates would provide important guidelines for optimization of important parameters, such as size and porosity. The results in this work showed that protein contained in taro starch native granules played an important role. It is postulated that protein acted as a bonding agent, cementing the spherical geometry obtained as a consequence of minimization of free energy in the spray-drying process. In the absence of protein, spherical aggregates would be unstable, leading to fast disaggregation after drying. FTIR analysis showed that protein contained on the granule surface underwent structural changes, which presumably can be linked to bonding effects. In fact, the increased presence of random secondary structures was found to parallel the stabilization of spherical aggregates. Spray-drying is a fast process taking place at temperatures above 100 °C. Typically, proteins denatures at temperatures below 100 °C.[24] In this way, the spray-drying process of starch granules allowed a fast, probably partial, melting of surface proteins, which allowed the bonding between starch granules. This effect, detected by FTIR analysis, would be the main mechanisms involved in the formation of spherical aggregates of starch granules.

It could be argued that surface protein can act as a barrier for the hydrolytic action of amylolytic enzymes. However, the results in Figure 7 and Table 1 showed the opposite result. In fact, the results indicated that the amount of protein is not sufficient for forming a stable surface layer for blocking the action of amylolytic enzymes. Rather, it seems that surface protein reduced the transfer of heat into the starch granule. The results showed that the thermal effects, reflected by FTIR 1047/1022 intensity ratio, were more pronounced when the protein was removed by protease treatment. In fact, the 1047/1022 intensity ratio increased in the spray-drying process, and the increase was more pronounced for protease-treated starch granules. The 1047/1022 intensity ratio has been linked to ordering and short-term (e.g., double-helices) crystallinity of starch granules,[21] such that increased values would imply reductions in enzymatic hydrolysis due to hampered action of amylolytic enzymes. This causal effect between increased 1047/1022 intensity ratio and reduced starch digestibility was observed in the present study. In this way, the thermal modifications of the starch structure played a more important role in the in vitro digestibility properties that the surface protein content.

4. Conclusions

The endogenous protein of the taro starch played a central role in the spontaneous formation of spherical structures upon spray-drying. The disruption of the taro starch protein by proteolysis reactions had an important negative effect on the formation of particle aggregates, which became less numerous, and showed irregular shapes. The formation of protein random structures seems to be at the center of the binding effect, which holds together the starch particles to form spherical aggregates. The detailed mechanism involved in the formation of spherical aggregates is not clear at all, and deserves a more in-depth study. On the other hand, spherical aggregates showed reduced digestibility compared to native taro starch. The effect might be ascribed to reduced exposed surface of spherical aggregates and to the enhanced molecular ordering induced by thermal shocks during spray-drying, which in turn limit the effectiveness of amylolytic enzymes. The results in the present study should help food processors to tailor the digestibility properties of starch aggregates used for microencapsulation for specific applications. By modulating the combined effect of spray-drying and added protease, protein contents can be altered, which in turn affects the production of starch structures with specific digestibility properties.

Conflict of Interest

The authors declare no conflict of interest.

Keywords

in vitro digestibility, protease, protein, spherical aggregates, taro starch

Received: March 23, 2019
Revised: May 13, 2019
Published online:

[1] J. Zhao, R. L. Whistler, *Cereal Chem.* **1994**, *71*, 392.
[2] J. Zhao, R. L. Whistler, *Food Technol.* **1994**, *48*, 104.
[3] T. A. Tari, U. S. Annapure, R. S. Singhal, P. R. Kulkarni, *Carbohydr. Polym.* **2003**, *53*, 45.
[4] S. Beirão-da-Costa, C. Duarte, M. Moldão-Martins, M. L. Beirão-da-Costa, *J. Food Eng.* **2011**, *104*, 36.
[5] R. A. Gonzalez-Soto, B. de la Vega, F. J. García-Suarez, E. Agama-Acevedo, L. A. Bello-Pérez, *LWT - Food Sci. Technol.* **2011**, *44*, 2064.
[6] J. Hoyos-Leyva, L. A. Bello-Pérez, E. Agama-Acevedo, J. Alvarez-Ramirez, *Int. J. Biol. Macromol.* **2018**, *120*, 237.
[7] X. Z. Han, B. R. Hamaker, *Cereal Chem. J.*. **2002**, *79*, 892.
[8] M. R. Debet, M. J. Gidley, *J. Agric. Food Chem.* **2007**, *55*, 4752.
[9] B. Zhang, S. Dhital, B. M. Flanagan, M. J. Gidley, *J. Agric. Food Chem.* **2014**, *62*, 760.
[10] I. Reyes, C. Hernandez-Jaimes, M. Meraz, M. E. Rodríguez-Huezo, *Rev. Mex. Ing. Quim.* **2018**, *17*, 279.
[11] H. M. Palma-Rodriguez, E. Agama-Acevedo, R. A. Gonzalez-Soto, E. J. Vernon-Carter, J. Alvarez-Ramirez, L. A. Bello-Perez, *Starch* **2013**, *65*, 584.
[12] I. Goñi, A. García-Alonso, F. Saura-Calixto, *Nutr. Res.* **1997**, *17*, 427.
[13] M. Hirai, K. Nakamura, T. Imai, T. Sato, *Jpn. J. Genet.* **1993**, *68*, 229.
[14] M. Hirai, T. Sato, K. Takayanagi, *Ikushugaku Zasshi* **1989**, *39*, 307.
[15] P. R. Pereira, E. M. Del Aguila, M. A. Verícimo, R. B. Zingali, V. M. F. Paschoalin, J. T. Silva, *Protein J.* **2014**, *33*, 92.
[16] M. C. Tang, L. Copeland, *Carbohydr. Polym.* **2007**, *67*, 80.
[17] R. Cui, C. G. Oates, *Food Chem.* **1999**, *65*, 417.
[18] B. Svihus, A. K. Uhlen, O. M. Harstad, *Anim. Feed Sci. Technol.* **2005**, *122*, 303.
[19] S. Simsek, M. Ovando-Martinez, A. Marefati, M. Rayner, *Food Res. Int.* **2015**, *75*, 41.
[20] H. Zaleska, S. Ring, P. Tomasik, *Carbohydr. Polym.* **2001**, *45*, 89.
[21] J. J. van Soest, H. Tournois, D. de Wit, J. F. Vliegenthart, *Carbohydr. Res.* **1995**, *279*, 201.
[22] F. Zeng, S. Zhu, F. Chen, Q. Gao, S. Yu, *Food Hydrocolloids* **2016**, *52*, 721.
[23] J. Ye, X. Hu, S. Luo, D. J. McClements, L. Liang, C. Liu, *Food Res. Int.* **2018**, *106*, 404.
[24] L. Smeller, *Biochim. Biophys. Acta, Protein Struct. Mol. Enzymol.* **2002**, *1595*, 11.